

# Chemical Genomics Identifies the Unfolded Protein Response as a Target for Selective Cancer Cell Killing during Glucose Deprivation

Sakae Saito,<sup>1</sup> Aki Furuno,<sup>1</sup> Junko Sakurai,<sup>1</sup> Asami Sakamoto,<sup>1</sup> Hae-Ryong Park,<sup>3</sup> Kazuo Shin-ya,<sup>2</sup> Takashi Tsuruo,<sup>1</sup> and Akihiro Tomida<sup>1</sup>

<sup>1</sup>Cancer Chemotherapy Center, Japanese Foundation for Cancer Research; <sup>2</sup>Biological Information Research Center, National Institute of Advanced Industrial Science and Technology, Tokyo, Japan and <sup>3</sup>Department of Food Science and Biotechnology, Kyungnam University, Masan, Korea

## Abstract

**Glucose deprivation, a cell condition that occurs in solid tumors, activates the unfolded protein response (UPR). A key feature of the UPR is the transcription program activation, which allows the cell to survive under stress conditions. Here, we show that the UPR transcription program is disrupted by the antidiabetic biguanides metformin, buformin, and phenformin depending on cellular glucose availability. These drugs inhibit production of the UPR transcription activators XBP1 and ATF4 and induce massive cell death during glucose deprivation as did the antitumor macrocyclic compound versipelostatatin. Gene expression profiling shows remarkable similarity in the modes of action of biguanides and versipelostatatin determined by the broad range of glucose deprivation-inducible genes. Importantly, during glucose deprivation, most of the biguanide suppression genes overlap with the genes induced by tunicamycin, a chemical UPR inducer. Gene expression profiling also identifies drug-driven signatures as a tool for discovering pharmacologic UPR modulators. Our findings show that disrupting the UPR during glucose deprivation could be an attractive approach for selective cancer cell killing and could provide a chemical genomic basis for developing UPR-targeting drugs against solid tumors.** [Cancer Res 2009;69(10):4225–34]

## Introduction

Cell conditions that lead to the accumulation of misfolded or unfolded proteins in the endoplasmic reticulum (ER) activate the unfolded protein response (UPR; refs. 1, 2). The UPR is a complex signaling network that enhances cell survival by limiting the accumulation of unfolded or misfolded proteins in the ER (1, 2). A key feature of the UPR is its transcription program activation, which is initiated through signaling of the ER-localized transmembrane proteins ATF6, PKR-like ER kinase (PERK), and inositol-requiring 1 (IRE1; refs. 1, 2). These ER stress sensor proteins produce several different active transcription factors. ATF6 becomes an active transcription factor by proteolytic cleavage (3, 4), whereas IRE1 mediates the unconventional splicing of XBP1 mRNA, thereby converting it to a potent UPR transcriptional activator (5–8). PERK induces the transcription factor ATF4 by phosphorylating eIF2 $\alpha$  and transiently inhibiting general protein synthesis (9–11). These

transcription factors lead to coordinated induction of divergent UPR target genes, such as the ER-resident molecular chaperones glucose-regulated protein 78 (GRP78) and 94 (GRP94), for cell survival (12, 13). In the case of intolerable levels of ER stress, however, the sensor proteins can contribute to eliciting apoptosis (1, 2).

One of the major physiologic cell conditions leading to UPR activation is glucose deprivation, which is associated with several human diseases including tissue ischemia and cancer (14). The UPR is thought to protect tumor cells from the stressful conditions of glucose deprivation and hypoxia as well as from immune surveillance (12, 15). Consistently, the elevated levels of GRP78 are seen in a variety of cancer cell lines, solid tumors, and human cancer biopsies and can be associated with lowered chemosensitivity in breast cancer and gliomas (16, 17). Thus, the UPR may be an important target by which to improve cancer chemotherapy. We recently isolated a novel macrocyclic compound, versipelostatatin, which shows highly selective cytotoxicity to glucose-deprived tumor cells and exerts *in vivo* antitumor activity (18). Versipelostatatin inhibits GRP78 induction and represses the production of the UPR transcription activators XBP1 and ATF4 during glucose deprivation. However, it is not known to what extent versipelostatatin affects the glucose deprivation-induced stress response to exert the selective cytotoxicity.

Gene expression profiling has been used to characterize the UPR in cell lines defective in such ER stress signaling genes as PERK, eIF2 $\alpha$ , ATF4, ATF6, and XBP1 (11, 19–21). Interestingly, each defect has a different effect on the UPR transcription program as well as on cell survival during ER stress, suggesting that gene expression profiling would be useful to define the nature of the perturbation induced by UPR-modulating compounds. Meanwhile, recent studies revealed that gene expression profiling can also be used in drug discovery. Notably, the Connectivity Map system has successfully identified functional similarity between seemingly diverse compounds by detecting similarities among gene expression profiles of cellular responses to a large number of bioactive compounds (22–24). Thus, gene expression profiling with UPR-modulating compounds may provide useful information for drug discovery.

In the course of screening for UPR modulators, we found that the antidiabetic biguanides metformin, buformin, and phenformin could inhibit activation of a GRP78 promoter reporter during glucose deprivation. Among these biguanides, metformin has been most widely used to treat type 2 diabetes (25, 26). Metformin lowers blood glucose levels probably by activating the AMP-activated protein kinase (AMPK; refs. 25, 26). In fact, metformin activates AMPK at millimolar levels in various cultured cells (27, 28). Recently, metformin was shown to exert antitumor effects *in vitro* and *in vivo* via AMPK-dependent and AMPK-independent pathways

**Note:** Supplementary data for this article are available at Cancer Research Online (<http://cancerres.aacrjournals.org/>).

**Requests for reprints:** Akihiro Tomida, Cancer Chemotherapy Center, Japanese Foundation for Cancer Research, 3-10-6 Ariake, Koto-ku, Tokyo 135-8550, Japan. Phone: 81-3-3570-0514; Fax: 81-3-3570-0484; E-mail: akihiro.tomida@jfcrr.or.jp.

©2009 American Association for Cancer Research.

doi:10.1158/0008-5472.CAN-08-2689

(27, 28). However, the underlying mechanisms are not fully understood. Here, we show that the antidiabetic biguanides, similar to versipelostatatin, modulate the UPR transcription program and induce cell death in glucose-deprived tumor cells. The modes of action of biguanides and versipelostatatin are very similar as shown on biochemical analysis and gene expression profiling. Furthermore, we show that the gene expression signatures, identified with biguanides and versipelostatatin, can be successfully used in discovery of novel UPR-targeting drugs.

## Materials and Methods

**Chemicals.** Versipelostatatin was prepared as a stock solution of 10 mmol/L in DMSO (18). Metformin (Sigma), phenformin (Sigma), buformin (Wako), and 2-deoxy-D-glucose (2DG; Sigma) were dissolved in sterilized distilled water at stock concentrations of 1 mol/L, 100 mmol/L, 100 mmol/L, and 2 mol/L, respectively. Tunicamycin (Nacalai Tesque), pyrvinium pamoate (MP Biomedicals), and MG132 (Peptide Institute) were dissolved in DMSO at stock concentrations of 4 mg/mL, 10 mmol/L, and 10 mmol/L, respectively. All the stock solutions were stored at  $-20^{\circ}\text{C}$ . DMSO represented  $<0.5\%$  of the medium volume.

**Cell lines and cell treatments.** Cells were maintained in RPMI 1640 (Nissui; for human colon cancer HT-29, fibrosarcoma HT1080, stomach cancer MKN74, and renal cell carcinoma 786-O) or DMEM (Nissui; for HeLa). Both media, containing 2 mg/mL glucose, were supplemented with 10% heat-inactivated fetal bovine serum and 100  $\mu\text{g}/\text{mL}$  kanamycin. All cell lines were cultured at  $37^{\circ}\text{C}$  in a humidified atmosphere containing 5%  $\text{CO}_2$  as the normal growth condition.

To induce the UPR, we treated cells for various times under ER stress conditions by replacing the medium with glucose-free medium or by adding either 2DG or tunicamycin to glucose-containing medium. The glucose-free RPMI 1640 and DMEM (Invitrogen) were supplemented with 10% heat-inactivated fetal bovine serum (29). Versipelostatatin, biguanides, or pyrvinium pamoate were added at various final concentrations immediately after cells were placed in glucose-free medium or just before the chemical stressors were added to glucose-containing culture medium. In some immunoblot analyses, we treated cells with the proteasome inhibitor MG132 at 10  $\mu\text{mol}/\text{L}$  during exposure to the UPR inducers.

**Cell viability assays.** For the 3-(4,5-dimethylthiazol-2-yl)-2,5-diphenyltetrazolium bromide assay, HeLa cells were cultured overnight in 96-well plates ( $3 \times 10^3$  per well) and then treated with various concentrations of versipelostatatin, biguanides, or pyrvinium pamoate in the presence or absence of 10 mmol/L 2DG or 1  $\mu\text{g}/\text{mL}$  tunicamycin as a stressor for 30 h.

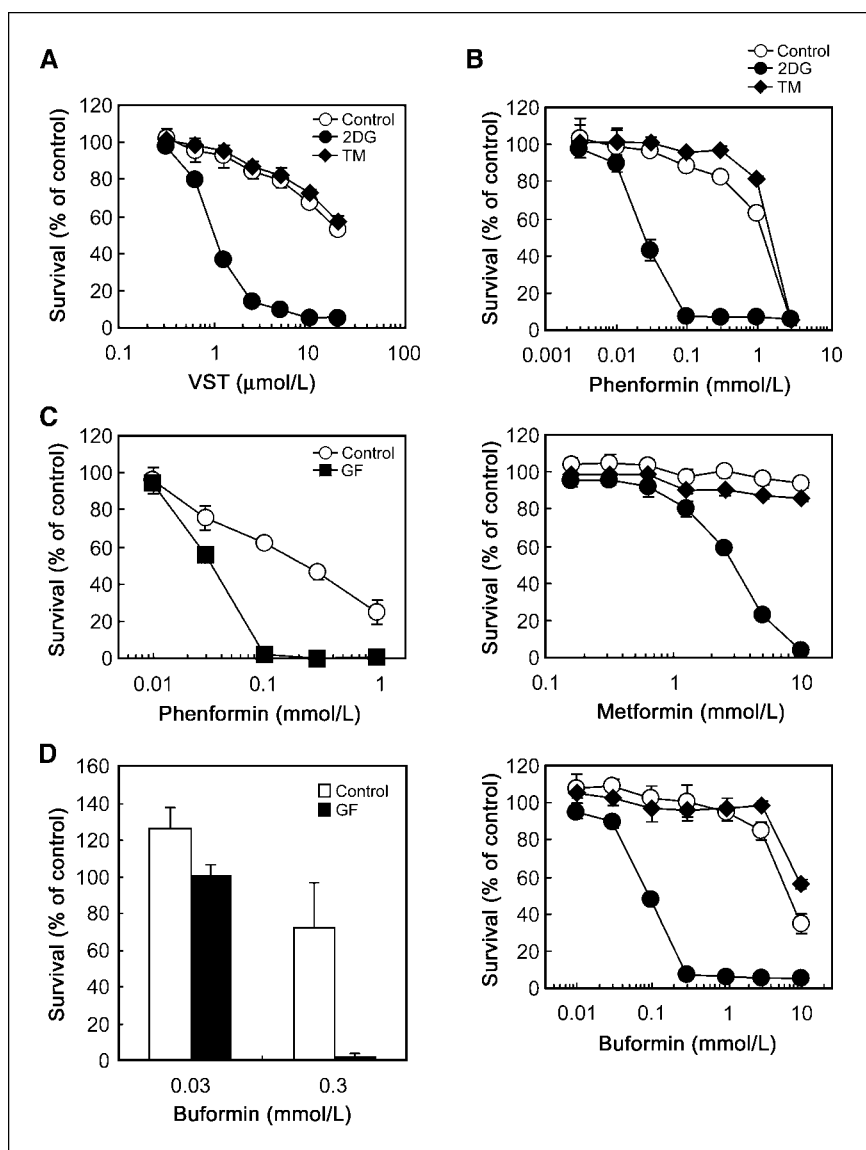


**Figure 1.** Selective cytotoxicity of biguanides against glucose-deprived cells. *A* and *B*, 3-(4,5-dimethylthiazol-2-yl)-2,5-diphenyltetrazolium bromide assay of HeLa cells treated with versipelostatatin (VST; *A*) or biguanides [*B*; phenformin (*top*), metformin (*middle*), and buformin (*bottom*)] under normal or ER stress conditions. 2DG, 10 mmol/L 2DG; TM, 1  $\mu\text{g}/\text{mL}$  tunicamycin. *C* and *D*, colony formation assay of HT-29 cells treated with phenformin (*C*) or buformin (*D*) in normal or glucose-free (GF) medium. Mean  $\pm$  SD.

The medium was then replaced with fresh growth medium, and cells were cultured for a further 15 h. Subsequently, 3-(4,5-dimethylthiazol-2-yl)-2,5-diphenyltetrazolium bromide (Sigma) was added to the culture medium, and the absorbance of each well was determined as described previously (30). Relative cell survival (mean  $\pm$  SD of quadruplicate determinations) was calculated by setting each of the control absorbance from non-drug-treated cells as 100%.

For the colony formation assay, HT-29 cells were cultured overnight in 24-well plates ( $4 \times 10^4$  per well) and then treated with various concentrations of phenformin or buformin in normal or glucose-free medium for 24 h. Cells were then diluted in fresh medium that lacked biguanides, reseeded, and cultured under normal growth conditions to form colonies as described previously (29). The cell viability (mean  $\pm$  SD of triplicate determinations) was calculated by setting each of the non-drug-treated cell survivals as 100%.

**Plasmids and transfection.** The pcFLAG vector, pGRP78pro160-Luc, and 7 $\times$  FLAG-tagged ATF6 have been described previously (18, 31). The FLAG-tagged XBP1-Luc plasmid was generated by ligating a FLAG-tagged coding sequence and human XBP1 splicing region into the *HindIII/ApaI* site of pGL4.13 plasmid vector (Promega) upstream of luciferase. The XBP1 splicing region encompassed nucleotides 410 to 633 relative to the start of transcription of the human XBP1 cDNA, including the 26-nucleotide ER stress-specific intron (5). The proper construction of plasmids was

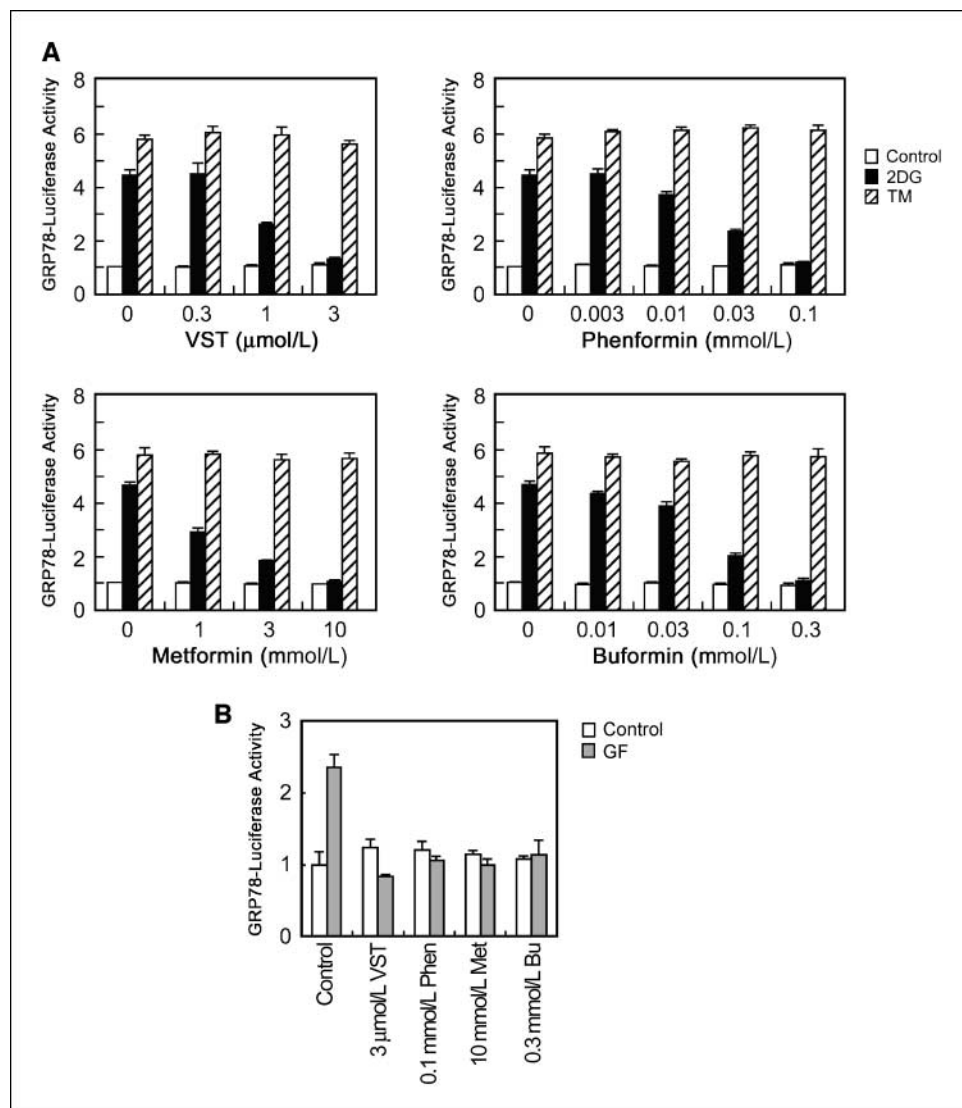
confirmed by DNA sequencing. Transient transfections were done using the FuGENE6 Transfection Reagent (Roche Molecular Biochemicals) with antibiotic-free RPMI 1640 supplemented with 5% fetal bovine serum according to the manufacturer's protocol.

**Reporter assay.** Reporter assay was done as described previously (ref. 18; see also Supplementary Methods). Briefly, HT1080 cells were transfected with firefly luciferase-containing reporter plasmids (pGRP78pro160-Luc or FLAG-tagged XBP1-Luc) and *Renilla* luciferase-containing plasmid phRL-CMV (Promega) as an internal control. Relative activity of firefly luciferase to *Renilla* luciferase (mean  $\pm$  SD of triplicate determinations) was determined using the Dual-Glo Luciferase Assay System (Promega).

**Immunoblot analysis.** Immunoblot analysis was done as described previously (ref. 18; see also Supplementary Methods). Briefly, equal amounts of proteins were resolved on a SDS-polyacrylamide gradient gel and transferred by electroblotting onto a nitrocellulose membrane. Membranes were probed with the indicated primary antibodies. The specific signals were visualized with a chemiluminescence detection system using appropriate secondary antibodies (Perkin-Elmer).

**Microarray expression profiles.** Microarray analysis was done according to standard Affymetrix protocols using GeneChip Human Genome U133 Plus 2.0 arrays (see also Supplementary Methods). The microarray data sets were deposited in the National Center for

**Figure 2.** Suppressive effect of biguanides on GRP78 promoter activity. HT1080 cells were transfected with pGRP78pro160-Luc and exposed to stress [10 mmol/L 2DG or 5  $\mu$ g/mL tunicamycin (A) or glucose withdrawal (B)] for 18 h with versipelostatin or biguanides. Mean  $\pm$  SD.



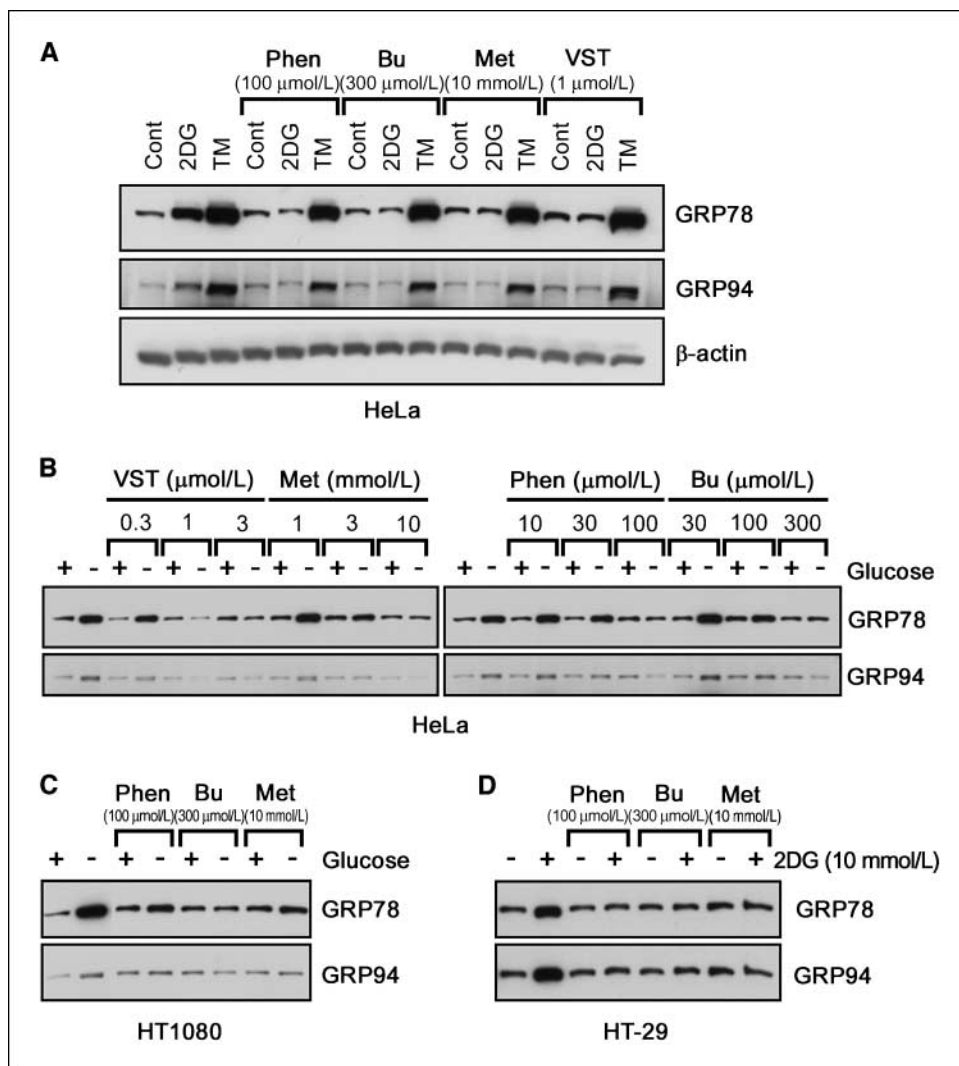


**Figure 3.** Selective inhibition of biguanides on GRP78 and GRP94 protein accumulation. Immunoblot analysis of GRP78 and GRP94. *A*, HeLa cells were treated for 15 h under normal or ER stress conditions (5 mmol/L 2DG or 1 μg/mL tunicamycin) with versipelostatatin or biguanides. *Bu*, buformin; *Met*, metformin; *Phen*, phenformin. β-Actin was used as a loading control. *B*, HeLa cells were treated for 15 h with versipelostatatin or biguanides in the presence (+) or absence (-) of glucose. HT1080 (*C*) and HT-29 (*D*) cells were treated for 18 h with versipelostatatin or biguanides in the presence or absence of glucose (*C*) or 10 mmol/L 2DG (*D*).

Biotechnology Information Gene Expression Omnibus<sup>4</sup> under the series accession no. GSE13548.

**Statistical analysis.** Normalization of microarray data was carried out by the Robust Multichip Average method using the RMAExpress version 1.0 (32). All microarray data were normalized within each set before Significance Analysis of Microarray (33). To select significant genes based on differential expression between the sets of interest, two class paired Significance Analysis of Microarray were done using the R package "samr."<sup>5</sup> In the glucose deprivation data set (including 16 samples) and the versipelostatatin/biguanide data set (including 10 samples), 2,253 and 118 significant probe sets were selected with false discovery rates of 0.5% and 20%, respectively. The list of paired sample data for each Significance Analysis of Microarray is provided in Supplementary Table S2. As the Glucose Deprivation signature, 246 of significant probe sets were selected with the fold change cutoff of >2-fold up and down. As the versipelostatatin/biguanide signature, 25 of significant probe sets were selected with the fold change cutoff of >2-fold up and >1.67-fold down. In the latter analysis, the cutoff value for fold change was set at 1.67-fold in the down-regulated genes because, for the 2-fold cutoff value, we could not obtain the probe sets (down tags) necessary for Connectivity Map analysis.

Unsupervised, hierarchical clustering of signature genes was done using Cluster 3.0 software and visualized with Java TreeView (34). Categorical annotation of genes was done by Gene Ontology, and significant enrichment for specific biological functional categories was identified using DAVID (35). The pattern-matching analysis of gene expression signatures was done using the Connectivity Map database build 02 (22).

## Results

**Cytotoxicity and UPR inhibition by biguanides during glucose deprivation.** To facilitate comparison of the cytotoxic activity of small compounds under normal and UPR-inducing stress conditions, we established a 3-(4,5-dimethylthiazol-2-yl)-2,5-diphenyltetrazolium bromide-based assay system using HeLa cells (Fig. 1). We used two different types of chemical UPR inducers, the hypoglycemia-mimicking agent 2DG and the *N*-glycosylation inhibitor tunicamycin. In agreement with our previous study (18), versipelostatatin showed selective cytotoxicity under 2DG stress conditions (Fig. 1A). Similarly, the antidiabetic biguanides phenformin, metformin, and buformin showed selective cytotoxicity under 2DG stress conditions (Fig. 1B). Notably, the IC<sub>50</sub> (concentration reducing cell survival by 50%) values of phenformin and buformin were ~30-fold lower under 2DG stress than under

<sup>4</sup> <http://www.ncbi.nlm.nih.gov/projects/geo/>

<sup>5</sup> <http://www-stat.stanford.edu/~tibs/SAM/index.html>

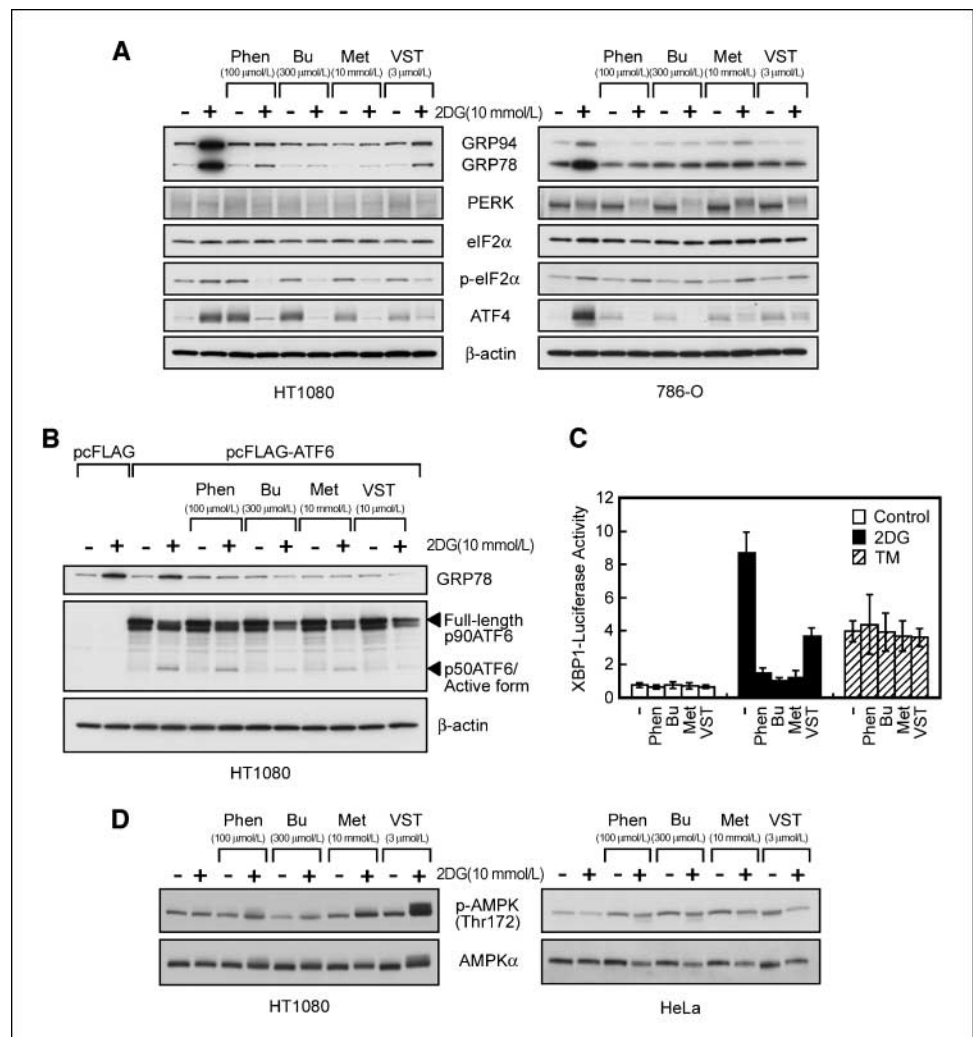
normal growth conditions. In contrast to 2DG, tunicamycin showed no combined effect of the biguanides. When colon cancer HT-29 cells were treated with phenformin and buformin in glucose-free medium, a similar sensitization to these biguanides occurred as shown by a colony formation assay (Fig. 1C and D).

We next compared the effects of biguanides and versipelostatin on human GRP78 promoter activity in HT1080 cells that were transiently transfected with the reporter gene plasmid pGRP78 pro160-Luc (18). As shown in Fig. 2A, treatments of the transfected cells with 2DG and tunicamycin increased GRP78 promoter activity by ~5- and 6-fold, respectively. Both biguanides and versipelostatin suppressed 2DG-induced GRP78 promoter activity in a dose-dependent manner but had little effect on tunicamycin-induced GRP78 promoter activity. The inhibition concentrations were the same ranges noted when cytotoxic activities were observed in 2DG-stressed HeLa cells (Fig. 1). Biguanides also suppressed GRP78 promoter activity induced by glucose withdrawal (Fig. 2B). The UPR-inhibitory activities of biguanides were also confirmed by immunoblot analysis of endogenous GRP78 and GRP94 (Fig. 3). Biguanides selectively and dose-dependently suppressed 2DG-induced GRP78 and GRP94 protein accumulation when HeLa cells were treated with 2DG or tunicamycin for 18 h in the presence or absence of biguanides (Fig. 3A and B). We saw similar results in

HT1080 during glucose withdrawal and in 2DG-stressed HT-29 cells (Fig. 3C and D). The UPR-inhibitory activities of both biguanides and versipelostatin were seen in cells stressed with either 2DG or glucose withdrawal.

**Effects of biguanides on upstream signaling pathways of the UPR.** We examined the effects of biguanides on the PERK-eIF2 $\alpha$ -ATF4 signaling pathway in HT1080 and 786-O cells that were stressed with 2DG for 18 h (Fig. 4A). Immunoblot analysis clearly detected 2DG-induced PERK activation in 786-O cells but less clearly in HT1080 cells as shown by phosphorylation-mediated band shifts (9). Adding biguanides as well as versipelostatin did not affect 2DG-induced PERK activation, although these compounds effectively suppressed GRP78 and GRP94 induction. The same treatments did not affect 2DG-induced enhancement in eIF2 $\alpha$  phosphorylation in 786-O cells but suppressed it in HT1080 cells. At the 6 h time point, however, 2DG-induced eIF2 $\alpha$  phosphorylation was not inhibited in HT1080 cells (see Supplementary Fig. S1). In contrast to the complicated response of eIF2 $\alpha$  phosphorylation, 2DG-induced ATF4 expression was consistently suppressed by biguanides and versipelostatin at either 6 or 18 h time point (Fig. 4A; Supplementary Fig. S1). Paradoxically, in the absence of 2DG, both biguanides and versipelostatin induced ATF4 protein accumulation.

**Figure 4.** Effects of biguanides on the UPR signaling pathway. *A, B, and D*, immunoblot analysis of UPR-related proteins. *A* and *D*, HT1080, 786-O, and HeLa cells were treated for 18 h with versipelostatin or biguanides in the presence or absence of 10 mmol/L 2DG. *B*, HT1080 cells were transfected with 100 ng of 7 $\times$  FLAG-tagged ATF6 plasmid (expressed FLAG-tagged full-length p90ATF6) and treated for 6 h with versipelostatin or biguanides in the presence or absence of 10 mmol/L 2DG. For better detection of p50ATF6/active form, MG132 was included during exposure of cells to 2DG.  $\beta$ -Actin was used as a loading control. *C*, XBP1 reporter assay. HT1080 cells were transfected with FLAG-tagged XBP1-Luc and exposed to stress (10 mmol/L 2DG or 5  $\mu$ g/mL tunicamycin) for 18 h with versipelostatin or biguanides.



We examined whether biguanides inhibited ATF6 and IRE1-XBP1 signaling pathways (Fig. 4B and C). First, HT1080 cells were transiently transfected with the plasmid of 7×FLAG-tagged ATF6, so that the ATF6 activation process was detected in a 2DG stress-dependent manner (Fig. 4B). Production of the p50ATF6/active form was somewhat decreased by biguanides as well as by versipelostatatin (Fig. 4B). Next, HT1080 cells were transiently transfected with a reporter plasmid encoding a fusion protein of a XBP-1 fragment and luciferase, which produces luciferase activity only when the 26 bp of the XBP-1 fragment mRNA is spliced out by IRE1 during ER stress. Treatments of the transfected cells with 2DG and tunicamycin increased luciferase activity from the fusion reporter by ~8- and 4-fold, respectively (Fig. 4C). Under normal growth conditions, biguanides and versipelostatatin suppressed 2DG-induced, but not tunicamycin-induced, reporter activity without affecting the basal activity (Fig. 4C). Collectively, these results indicated that biguanides and versipelostatatin exhibited very similar effects on upstream signaling pathways of the UPR depending on the glucose deprivation conditions.

The antidiabetic action of metformin has reportedly been associated with activation of AMPK (25, 26). We then examined the effects of biguanides and versipelostatatin on AMPK phosphorylation status in HT1080 and HeLa cells, the latter being negative for LKB1, an upstream kinase of AMPK (36, 37). As shown in Fig. 4D, combined treatments with 2DG and biguanides tended to enhance phosphorylation of AMPK in HT1080 cells, whereas the treatments tended to decrease levels of both total expression and AMPK phosphorylation in HeLa cells. An exception we observed was the strong AMPK phosphorylation enhancement in HT1080 cells treated with 2DG and versipelostatatin. Thus, biguanides and versipelostatatin showed less consistent effects on AMPK than on the UPR signaling pathways.

**Gene expression signature of glucose deprivation with UPR modulators.** We obtained gene expression profiles from four different cancer cell lines (HT1080, HT-29, HeLa, and MKN74) that were treated for 15 or 18 h with various combinations of stressors (glucose withdrawal, 2DG, or tunicamycin) and modulator compounds (biguanides or versipelostatatin; see Supplementary Table S1). The exposure periods were sufficient to activate the UPR but not long enough to cause apparent, overt cell death even in the presence of biguanides and versipelostatatin. We first identified an expression signature that captured the cellular response on glucose deprivation. Following the Significance Analysis of Microarray, 178 genes (246 probe sets), termed the Glucose Deprivation signature, were identified as differentially expressed genes that were either up-regulated (97 genes or 148 probe sets) or down-regulated (81 genes or 98 probe sets; Fig. 5A; Supplementary Table S3) by glucose withdrawal and 2DG. Analyzing 16 of 178 genes with real-time reverse transcription-PCR showed an excellent correlation between microarray and reverse transcription-PCR (see Supplementary Fig. S2). Categorical analysis of the up-regulated genes revealed enrichment of stress response and UPR-related categories, such as ER, unfolded protein binding, disulfide isomerase, and chaperone (see Supplementary Table S5). The 97 up-regulated genes also contained the UPR markers GRP78 and GRP94 and transcription factor XBP1 with relatively high scores. Categorical analysis of the 81 down-regulated genes revealed enrichment of cell cycle, cell division, and DNA replication categories (see Supplementary Table S5). The genes of the Glucose Deprivation signature in cells treated with tunicamycin, another UPR inducer, showed

expression change similar to cells treated with glucose deprivation (Fig. 5A; see also Supplementary Fig. S3). In the 148 up-regulated probe sets, 92 (62.2%) probe sets were also >2-fold up-regulated by tunicamycin-treatment (Fig. 5B). The 98 down-regulated probe sets were weakly influenced by tunicamycin, but 76 (77.6%) probe sets were >1.43-fold down-regulated.

As shown in the heat map, induction of the Glucose Deprivation signature genes was largely prevented when biguanides and versipelostatatin were added under 2DG stress or glucose withdrawal conditions (Fig. 5A). In the up-regulated 148 probe sets, induction of 81 (54.7%) probe sets were effectively inhibited (the inhibition efficiency >50%) in the presence of biguanide or versipelostatatin. By contrast, in the down-regulated 98 probe sets, most of the probe sets (92 probe sets, 93.9%) were just slightly affected by the addition of these compounds (Fig. 5C). In agreement with the marginal effect of versipelostatatin on the tunicamycin-induced UPR (see above), the expression patterns of the Glucose Deprivation signature genes were essentially the same between tunicamycin-treated cells in the presence or absence of versipelostatatin (Fig. 5A). Taken together, these results show that biguanides and versipelostatatin similarly and broadly modulate the transcription program of the stress response, especially the UPR during glucose deprivation.

**Gene expression signature-based identification of UPR modulators.** To investigate the utility of our gene expression data further, we employed the Connectivity Map, a software tool that searches for similarities between the expression signature of interest and a reference collection of expression profiles that were obtained from cell lines treated with various drugs (22). On querying the Connectivity Map, the Glucose Deprivation signature showed strong similarity to expression profiles of known UPR inducers, including 7-allylamino-17-demethoxygeldanamycin, ionomycin, 2DG, and MG132 (data not shown). To identify novel UPR inhibitors using the Connectivity Map, we next extracted from our microarray data a common expression signature of cells treated with biguanides and versipelostatatin under normal growth conditions (see Supplementary Fig. S4A; Supplementary Table S6). This signature consisted of 24 genes (25 probe sets), of which 10 genes (11 probe sets) overlapped with the Glucose Deprivation signature. The 9 up-regulated genes contained DDIT3/GADD153/CHOP, VEGFA, CEBPG, and TRB3, which are known as a downstream target of ATF4, consistent with the observation that ATF4 protein induction occurred in cells treated with versipelostatatin and biguanides under normal growth conditions (Fig. 4A). The Connectivity Map revealed similarity between the newly defined versipelostatatin/biguanide signature and the expression profiles of some bioactive drugs (see Supplementary Table S7).

Among those drugs, we focused on an antihelminthic pyriminium pamoate that showed a high-ranked match for the versipelostatatin/biguanide signature with high specificity in the Connectivity Map analysis regardless of whether we considered different cell lines (see Supplementary Fig. S4B; Supplementary Table S7). Besides, pyriminium pamoate has been reported to be more toxic under glucose starvation than under normal growth conditions and to exert antitumor activity against pancreatic cancer xenografts (38). However, little is known about its underlying mechanisms for selective toxicity against glucose-starved cells. To examine the effectiveness of the Connectivity Map-based screening, we tested whether pyriminium pamoate exerted selective toxicity and prevented the UPR during glucose deprivation. It did, indeed, show selective cytotoxicity to 2DG-stressed but not tunicamycin-stressed HeLa cells (Fig. 6A). The GRP78 promoter reporter assay in

HT1080 cells revealed that pyrvinium pamoate suppressed 2DG-induced but not tunicamycin-induced GRP78 promoter activity in a dose-dependent manner (Fig. 6B). Moreover, the effects of pyrvinium pamoate and versipelostatin on the Glucose Deprivation signature were quite similar in 2DG-stressed HT1080 cells (Fig. 6C). Consistently, pyrvinium pamoate selectively suppressed 2DG-induced and glucose withdrawal-induced GRP78, GRP94, and ATF4 protein accumulation in HT1080 cells (Fig. 6D), indicating that it was also the same class of UPR-modulating compound as versipelostatin.

## Discussion

We have characterized, herein, UPR-modulating activities of several compounds, including the antidiabetic biguanides metformin, buformin, and phenformin and an anthelmintic pyrvinium pamoate, in addition to versipelostatin. In spite of differences in chemical structure and known pharmacologic actions, these compounds similarly and broadly modulate the transcription

program of the 2DG- and glucose withdrawal-induced UPR as seen in the Glucose Deprivation signature. We noted that these compounds show selective cytotoxicity during glucose deprivation, indicating that modulation of the Glucose Deprivation signature is associated with cell death as a result of the drug treatment.

The common feature of these compounds is that the mode of action depends strictly on glucose deprivation. This raises the possibility that the UPR during glucose deprivation is governed by regulation mechanisms other than those initiated by the ER-transmembrane sensor proteins ATF6, IRE1, and PERK because these sensor proteins are commonly activated under glucose deprivation and tunicamycin stress conditions. Alternatively, the modes of action of the UPR-modulating drugs could differ depending on cellular glucose availability. Indeed, in the presence of glucose, biguanides as well as versipelostatin were able to induce the accumulation of an UPR transcription factor ATF4 protein, whereas they suppressed ATF4 induction during glucose deprivation (Fig. 4A). Because ATF4 induction occurs under different stress conditions (39), this observation raises the possibility

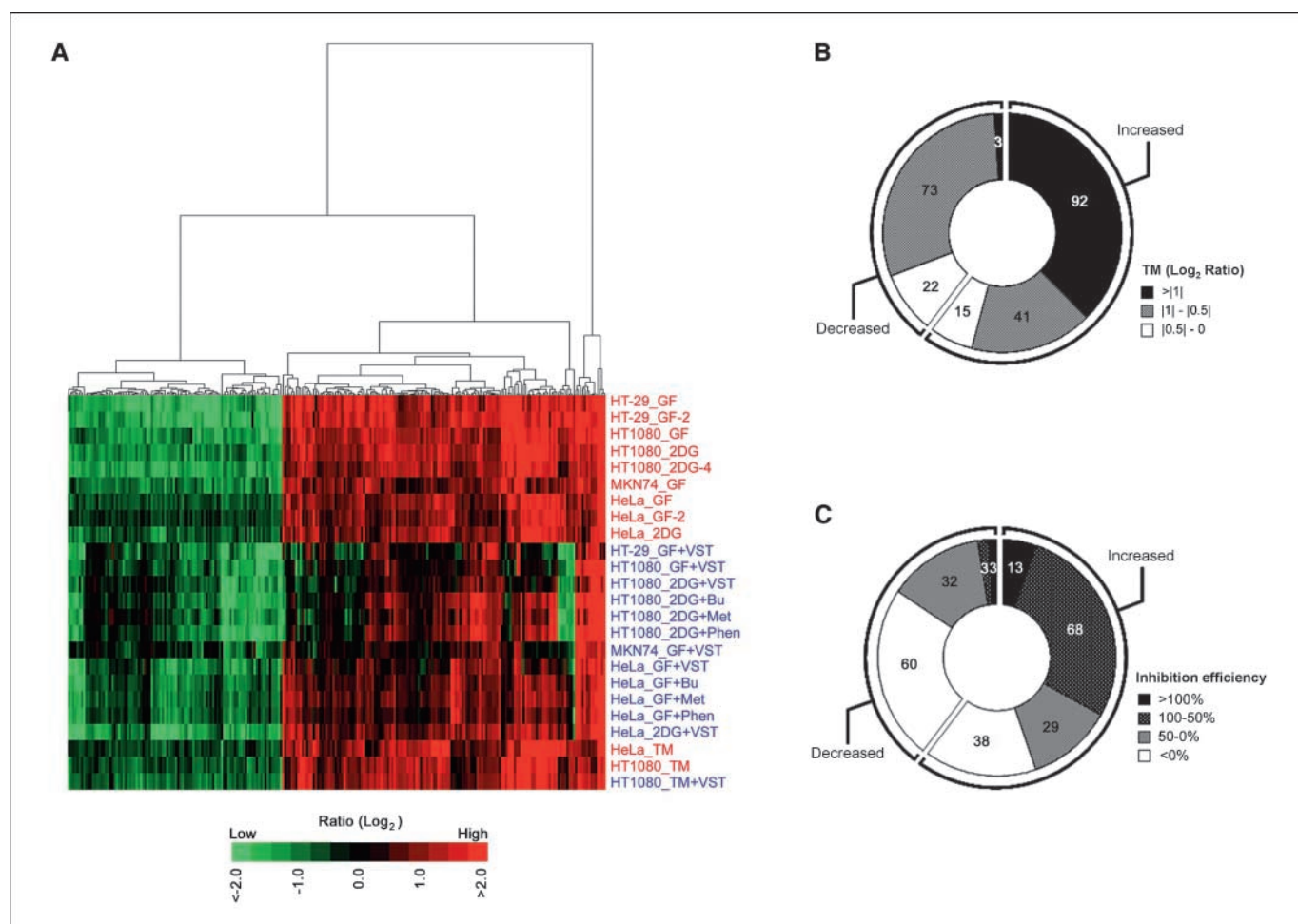


**Figure 5.** Prevention of glucose deprivation-induced gene expression by UPR modulators. **A**, Glucose Deprivation signature genes including 246 probe sets (*X* axis) sorted by cluster analysis displayed with 24 samples (*Y* axis). Cells were cultured for 15 to 18 h under normal growth condition (control), ER stress condition (red), or ER stress conditions with versipelostatin or biguanides (blue; see Supplementary Table S1 for detail). The log ratio for each gene was calculated by setting the expression level in appropriate control sample as 0 ( $\log_2 1$ ). **B**, effect of tunicamycin on Glucose Deprivation signature genes. The mean of expression change (log ratio) in tunicamycin-stimulated samples (without versipelostatin treatment) against control cells was calculated for each of 246 probe sets. **C**, effect of UPR modulators on Glucose Deprivation signature genes. The median of inhibition efficiency of the UPR modulators during glucose deprivation was expressed using the relative fold change ratio for each of 246 probe sets as determined by setting each 2DG-induced or glucose withdrawal-induced fold change in gene expression levels at 100%. In the pie charts (**B** and **C**), the number of probe sets is within each slice. *Increased*, up-regulated 148 probe sets; *Decreased*, down-regulated 98 probe sets of the Glucose Deprivation signature.

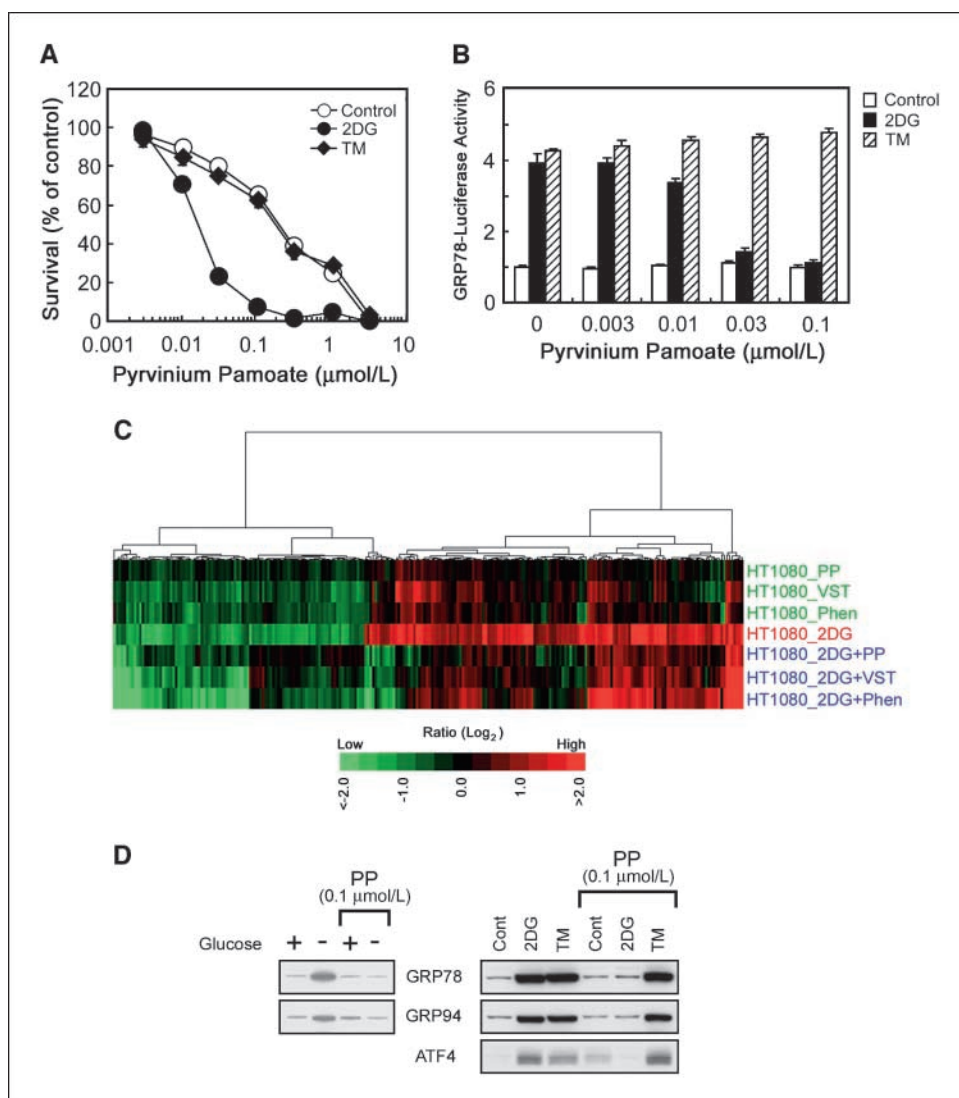


**Figure 6.** UPR modulator activity of pyrvinium pamoate. *A*, 3-(4,5-dimethylthiazol-2-yl)-2,5-diphenyltetrazolium bromide assay of HeLa cells treated with pyrvinium pamoate under ER stress conditions. *B*, GRP78 promoter reporter assay. HT1080 cells were transfected with pGRP78pro160-Luc plasmid and exposed to stress (10 mmol/L 2DG or 5  $\mu$ g/mL tunicamycin) for 18 h with pyrvinium pamoate. *C*, Glucose Deprivation signature genes including 246 probe sets (*X* axis) sorted by cluster analysis displayed with 7 samples (*Y* axis). HT1080 cells were cultured for 18 h with or without UPR modulators [pyrvinium pamoate (*PP*), versipelostatatin, and phenformin] under normal growth conditions (*green*) or under 2DG stress conditions (*blue* or *red*; see Supplementary Table S1 for detail). The log ratio for each gene was calculated by setting the expression level in appropriate control sample as 0 ( $\log_2 1$ ). *D*, immunoblot analysis of GRP78, GRP94, and ATF4. HT1080 cells were treated for 18 h with pyrvinium pamoate in the presence or absence of glucose (*left*) or chemical stressors (*right*).

that biguanides and versipelostatatin could stimulate another stress signaling pathway(s). In turn, ATF4 induction may explain why parts of the UPR target genes, such as DDIT3/GADD153/CHOP, VEGFA, CEBPG, and TRB3, were induced by these drugs under normal growth conditions.

It has been reported that the antidiabetic action of biguanides is associated with activation of the LKB1-AMPK signaling pathway (36, 37). However, the LKB1-AMPK pathway seems not to be essential in order for the drugs to modulate the UPR transcription program during glucose deprivation. Indeed, these drugs disrupted the UPR and exerted cytotoxic activity during glucose deprivation even in HeLa cells that are LKB1 defective. In addition, we showed that AMPK regulation in response to biguanides under 2DG stress conditions appeared to be different in HeLa and HT1080 cells (Fig. 4*D*), although UPR inhibition was commonly seen in both cell lines. Nevertheless, it is possible that the LKB1-AMPK pathway plays a role in cell survival during glucose deprivation. It is important to note that the cellular functions of AMPK show considerable overlap with those of the UPR. AMPK, which can be activated during glucose deprivation (25, 40, 41), induces down-regulation of protein translation and cell division processes, which

is also seen as the protective cellular response to UPR activation (2). Thus, the LKB1-AMPK pathway may enhance or compensate for the protective role of the UPR, especially when the UPR is suppressed. HeLa cells consistently exhibited hypersensitivity to cytotoxic action of biguanides and versipelostatatin during glucose deprivation, so it was necessary to reduce the concentrations of these compounds in the microarray analysis compared with HT1080 cell analysis (see Supplementary Table S1).

Recent advances in chemical genomics have revealed that a gene expression signature is useful for drug discovery, even when molecular targets or biochemical mechanisms of drugs are unclear (22–24). In this regard, the present study succeeded in identifying two types of gene expression signatures, the Glucose Deprivation signature and the versipelostatatin/biguanide signature that could be used in Connectivity Map-assisted drug discovery. The versipelostatatin/biguanide signature can be applied for compounds that cause cytotoxic modulation of the UPR during glucose deprivation as proven by experimentation with pyrvinium pamoate (Fig. 6). This was further supported by a recent report showing that pyrvinium pamoate suppressed the UPR in certain cell lines under glucose withdrawal conditions (42). At present, it is not known whether

there are common molecular targets of pyruvium pamoate, biguanides, and versipelostatin that could disrupt the UPR transcription program, thus indicating the usefulness of the gene expression signature-based drug discovery approach. Further support of the versipelostatin/biguanide signature usefulness is the finding that, according to Connectivity Map analysis, a potassium ionophore valinomycin and a protein kinase C inhibitor, rottlerin, were the high-ranked candidates for UPR-modulating compounds (see Supplementary Table S6). In fact, during the course of this study, valinomycin was shown to exert selective cytotoxicity to 2DG-treated cancer cells through down-regulation of GRP78 (43), and rottlerin was shown to suppress ER stress-induced autophagy, which is required for survival in response to ER stress (44).

It is likely that disrupting the UPR transcription program during glucose deprivation would be an attractive approach to cancer treatment. In fact, glucose deprivation as well as hypoxia are common features in poorly vascularized solid tumors but not observed in normal tissue, thereby providing a rationale for disrupting the UPR as a selective cancer therapy. Important to note is that versipelostatin, metformin, phenformin, and pyruvium pamoate exert antitumor activity in xenograft models (18, 38, 45, 46). Although relative high concentrations of biguanides were required to inhibit the UPR, they are in the same range as those needed to activate AMPK in cultured cells (27, 28). The AMPK activation is thought to play an important role in the antidiabetic affects of biguanides. Interestingly, metformin treatment in patients with type 2 diabetes has been associated with a lower

risk of cancer (47, 48). Thus, UPR-disrupting compounds would be interesting anticancer agent candidates. Meanwhile, depending on the type of tumor, compounds that induce the UPR can also be used as anticancer agents, for example, the proteasome inhibitor bortezomib and the HSP90 inhibitor geldanamycin analogues (49, 50). In these scenarios, the gene expression signatures identified in this study may be useful for drug discovery of both UPR-suppressing and UPR-inducing anticancer agents. Not limited to drug discovery, the gene expression signatures can support the drug development process as biomarkers. In addition to cancer, the UPR has recently been reported to be associated with neurodegenerative diseases, obesity, and diabetes (1). The present findings, therefore, could contribute to the development of UPR-targeting therapy against cancer and other UPR-involved conditions.

## Disclosure of Potential Conflicts of Interest

No potential conflicts of interest were disclosed.

## Acknowledgments

Received 7/14/08; revised 2/23/09; accepted 3/10/09.

**Grant support:** Ministry of Health, Labour and Welfare Grant-in-Aid for Cancer Research (15-2; A. Tomida) and Ministry of Education, Culture, Sports, Science and Technology of Japan Grant-in-Aid for Scientific Research on Priority Areas for Cancer (T. Tsuruo) and Grant-in-Aid for Young Scientists (B; 20790217; S. Saito).

The costs of publication of this article were defrayed in part by the payment of page charges. This article must therefore be hereby marked *advertisement* in accordance with 18 U.S.C. Section 1734 solely to indicate this fact.

We thank M. Ushijima and Dr. M. Matsuura (The Cancer Institute, JFCR) for helpful comments on the statistical analysis of microarray data.

## References

- Schroder M, Kaufman RJ. The mammalian unfolded protein response. *Annu Rev Biochem* 2005;74:739–89.
- Ron D, Walter P. Signal integration in the endoplasmic reticulum unfolded protein response. *Nat Rev Mol Cell Biol* 2007;8:519–29.
- Haze K, Yoshida H, Yanagi H, Yura T, Mori K. Mammalian transcription factor ATF6 is synthesized as a transmembrane protein and activated by proteolysis in response to endoplasmic reticulum stress. *Mol Biol Cell* 1999;10:3787–99.
- Yoshida H, Okada T, Haze K, et al. ATF6 activated by proteolysis binds in the presence of NF-Y (CBF) directly to the *cis*-acting element responsible for the mammalian unfolded protein response. *Mol Cell Biol* 2000;20:6755–67.
- Yoshida H, Matsui T, Yamamoto A, Okada T, Mori K. XBP1 mRNA is induced by ATF6 and spliced by IRE1 in response to ER stress to produce a highly active transcription factor. *Cell* 2001;107:881–91.
- Shen X, Ellis RE, Lee K, et al. Complementary signaling pathways regulate the unfolded protein response and are required for *C. elegans* development. *Cell* 2001;107:893–903.
- Calfon M, Zeng H, Urano F, et al. IRE1 couples endoplasmic reticulum load to secretory capacity by processing the XBP-1 mRNA. *Nature* 2002;415:92–6.
- Lee K, Tirasophon W, Shen X, et al. IRE1-mediated unconventional mRNA splicing and S2P-mediated ATF6 cleavage merge to regulate XBP1 in signaling the unfolded protein response. *Genes Dev* 2002;16:452–66.
- Harding HP, Zhang Y, Ron D. Protein translation and folding are coupled by an endoplasmic-reticulum-resident kinase. *Nature* 1999;397:271–4.
- Harding HP, Zhang Y, Bertolotti A, Zeng H, Ron D. Perk is essential for translational regulation and cell survival during the unfolded protein response. *Mol Cell* 2000;5:897–904.
- Harding HP, Zhang Y, Zeng H, et al. An integrated stress response regulates amino acid metabolism and resistance to oxidative stress. *Mol Cell* 2003;11:619–33.
- Dong D, Ni M, Li J, et al. Critical role of the stress chaperone GRP78/BiP in tumor proliferation, survival, and tumor angiogenesis in transgene-induced mammary tumor development. *Cancer Res* 2008;68:498–505.
- Fu Y, Lee AS. Glucose regulated proteins in cancer progression, drug resistance and immunotherapy. *Cancer Biol Ther* 2006;5:741–4.
- Semenza GL. Angiogenesis in ischemic and neoplastic disorders. *Annu Rev Med* 2003;54:17–28.
- Tomida A, Tsuruo T. Drug resistance mediated by cellular stress response to the microenvironment of solid tumors. *Anticancer Drug Des* 1999;14:169–77.
- Pyrko P, Schonthal AH, Hofman FM, Chen TC, Lee AS. The unfolded protein response regulator GRP78/BiP as a novel target for increasing chemosensitivity in malignant gliomas. *Cancer Res* 2007;67:9809–16.
- Lee E, Nichols P, Spicer D, Groshen S, Yu MC, Lee AS. GRP78 as a novel predictor of responsiveness to chemotherapy in breast cancer. *Cancer Res* 2006;66:7849–53.
- Park HR, Tomida A, Sato S, et al. Effect on tumor cells of blocking survival response to glucose deprivation. *J Natl Cancer Inst* 2004;96:1300–10.
- Lee AH, Iwakoshi NN, Glimcher LH. XBP-1 regulates a subset of endoplasmic reticulum resident chaperone genes in the unfolded protein response. *Mol Cell Biol* 2003;23:7448–59.
- Scheuner D, Song B, McEwen E, et al. Translational control is required for the unfolded protein response and *in vivo* glucose homeostasis. *Mol Cell* 2001;7:1165–76.
- Wu J, Rutkowski DT, Dubois M, et al. ATF6 $\alpha$  optimizes long-term endoplasmic reticulum function to protect cells from chronic stress. *Dev Cell* 2007;13:351–64.
- Lamb J, Crawford ED, Peck D, et al. The Connectivity Map: using gene-expression signatures to connect small molecules, genes, and disease. *Science* 2006;313:1929–35.
- Hieronymus H, Lamb J, Ross KN, et al. Gene expression signature-based chemical genomic prediction identifies a novel class of HSP90 pathway modulators. *Cancer Cell* 2006;10:321–30.
- Wei G, Twomey D, Lamb J, et al. Gene expression-based chemical genomics identifies rapamycin as a modulator of MCL1 and glucocorticoid resistance. *Cancer Cell* 2006;10:331–42.
- Kahn BB, Alquier T, Carling D, Hardie DG. AMP-activated protein kinase: ancient energy gauge provides clues to modern understanding of metabolism. *Cell Metab* 2005;1:15–25.
- Zhou G, Myers R, Li Y, et al. Role of AMP-activated protein kinase in mechanism of metformin action. *J Clin Invest* 2001;108:1167–74.
- Dowling RJ, Zakikhani M, Fantus IG, Pollak M, Sonenberg N. Metformin inhibits mammalian target of rapamycin-dependent translation initiation in breast cancer cells. *Cancer Res* 2007;67:10804–12.
- Sahra IB, Laurent K, Loubat A, et al. The antidiabetic drug metformin exerts an antitumoral effect *in vitro* and *in vivo* through a decrease of cyclin D1 level. *Oncogene* 2008;27:3576–86.
- Ogiso Y, Tomida A, Lei S, Omura S, Tsuruo T. Proteasome inhibition circumvents solid tumor resistance to topoisomerase II-directed drugs. *Cancer Res* 2000;60:2429–34.
- Denizot F, Lang R. Rapid colorimetric assay for cell growth and survival. Modifications to the tetrazolium dye procedure giving improved sensitivity and reliability. *J Immunol Methods* 1986;89:271–7.
- Tsukumo Y, Tomida A, Kitahara O, et al. Nucleobindin I controls the unfolded protein response by inhibiting ATF6 activation. *J Biol Chem* 2007;282:29264–72.
- Irizarry RA, Hobbs B, Collin F, et al. Exploration, normalization, and summaries of high density

- oligonucleotide array probe level data. *Biostatistics* 2003;4:249–64.
33. Tusher VG, Tibshirani R, Chu G. Significance analysis of microarrays applied to the ionizing radiation response. *Proc Natl Acad Sci U S A* 2001;98:5116–21.
  34. de Hoon MJ, Imoto S, Nolan J, Miyano S. Open source clustering software. *Bioinformatics* 2004;20:1453–4.
  35. Dennis G, Jr., Sherman BT, Hosack DA, et al. DAVID: Database for Annotation, Visualization, and Integrated Discovery. *Genome Biol* 2003;4:P3.
  36. Shaw RJ, Kosmatka M, Bardeesy N, et al. The tumor suppressor LKB1 kinase directly activates AMP-activated kinase and regulates apoptosis in response to energy stress. *Proc Natl Acad Sci U S A* 2004;101:3329–35.
  37. Shaw RJ, Lamia KA, Vasquez D, et al. The kinase LKB1 mediates glucose homeostasis in liver and therapeutic effects of metformin. *Science* 2005;310:1642–6.
  38. Esumi H, Lu J, Kurashima Y, Hanaoka T. Antitumor activity of pyruvium pamoate, 6-(dimethylamino)-2-[2-(2,5-dimethyl-1-phenyl-1H-pyrrol-3-yl)ethenyl]-1-methyl-quinolinium pamoate salt, showing preferential cytotoxicity during glucose starvation. *Cancer Sci* 2004;95:685–90.
  39. Rutkowski DT, Kaufman RJ. All roads lead to ATF4. *Dev Cell* 2003;4:442–4.
  40. Salt IP, Johnson G, Ashcroft SJ, Hardie DG. AMP-activated protein kinase is activated by low glucose in cell lines derived from pancreatic  $\beta$  cells, and may regulate insulin release. *Biochem J* 1998;335:533–9.
  41. Inoki K, Zhu T, Guan KL. TSC2 mediates cellular energy response to control cell growth and survival. *Cell* 2003;115:577–90.
  42. Yu DH, Macdonald J, Liu G, et al. Pyruvium targets the unfolded protein response to hypoglycemia and its anti-tumor activity is enhanced by combination therapy. *PLoS ONE* 2008;3:e3951.
  43. Ryoo IJ, Park HR, Choo SJ, et al. Selective cytotoxic activity of valinomycin against HT-29 human colon carcinoma cells via down-regulation of GRP78. *Biol Pharm Bull* 2006;29:817–20.
  44. Ozpolat B, Akar U, Mehta K, Lopez-Berestein G. PKC $\delta$  and tissue transglutaminase are novel inhibitors of autophagy in pancreatic cancer cells. *Autophagy* 2007;3:480–3.
  45. Schneider MB, Matsuzaki H, Haorah J, et al. Prevention of pancreatic cancer induction in hamsters by metformin. *Gastroenterology* 2001;120:1263–70.
  46. Dilman VM, Anisimov VN. Potentiation of antitumor effect of cyclophosphamide and hydrazine sulfate by treatment with the antidiabetic agent, 1-phenylethylbiguanide (phenformin). *Cancer Lett* 1979;7:357–61.
  47. Evans JM, Donnelly LA, Emslie-Smith AM, Alessi DR, Morris AD. Metformin and reduced risk of cancer in diabetic patients. *BMJ* 2005;330:1304–5.
  48. Bowker SL, Majumdar SR, Veugelers P, Johnson JA. Increased cancer-related mortality for patients with type 2 diabetes who use sulfonylureas or insulin. *Diabetes Care* 2006;29:254–8.
  49. Obeng EA, Carlson LM, Gutman DM, Harrington WJ, Jr., Lee KP, Boise LH. Proteasome inhibitors induce a terminal unfolded protein response in multiple myeloma cells. *Blood* 2006;107:4907–16.
  50. Davenport EL, Moore HE, Dunlop AS, et al. Heat shock protein inhibition is associated with activation of the unfolded protein response pathway in myeloma plasma cells. *Blood* 2007;110:2641–9.

# Cancer Research

The Journal of Cancer Research (1916–1930) | The American Journal of Cancer (1931–1940)

## Chemical Genomics Identifies the Unfolded Protein Response as a Target for Selective Cancer Cell Killing during Glucose Deprivation

Sakae Saito, Aki Furuno, Junko Sakurai, et al.

*Cancer Res* 2009;69:4225-4234. Published OnlineFirst May 12, 2009.

### Updated version

Access the most recent version of this article at:  
doi:[10.1158/0008-5472.CAN-08-2689](https://doi.org/10.1158/0008-5472.CAN-08-2689)

### Supplementary Material

Access the most recent supplemental material at:  
<http://cancerres.aacrjournals.org/content/suppl/2009/04/27/0008-5472.CAN-08-2689.DC1>

### Cited articles

This article cites 50 articles, 22 of which you can access for free at:  
<http://cancerres.aacrjournals.org/content/69/10/4225.full.html#ref-list-1>

### Citing articles

This article has been cited by 10 HighWire-hosted articles. Access the articles at:  
</content/69/10/4225.full.html#related-urls>

### E-mail alerts

[Sign up to receive free email-alerts](#) related to this article or journal.

### Reprints and Subscriptions

To order reprints of this article or to subscribe to the journal, contact the AACR Publications Department at [pubs@aacr.org](mailto:pubs@aacr.org).

### Permissions

To request permission to re-use all or part of this article, contact the AACR Publications Department at [permissions@aacr.org](mailto:permissions@aacr.org).